Single-Molecule Femtochemistry: Molecular Imaging at the Space-Time Limit

Hrvoje Petek*

Department of Physics and Astronomy, University of Pittsburgh, Pittsburgh, Pennsylvania 15260, United States

ABSTRACT Through a combination of light and electron probes, it may be possible to record single-molecule dynamics with simultaneous sub-Ångstrom spatial and femtosecond temporal resolution. Single-molecule femtochemistry is becoming a realistic prospect through a melding of laser spectroscopy and electron microscopy techniques. The paper by Lee *et al.* in this issue of *ACS Nano* takes a significant step toward chemical imaging at the space-time limit of chemical processes. By imaging electroluminescence spectra of single porphyrin molecules with submolecular resolution, the authors extract the implicit femtosecond dynamics of the coupled electron orbital–molecular skeletal motion triggered by a reduction–oxidation scattering process.

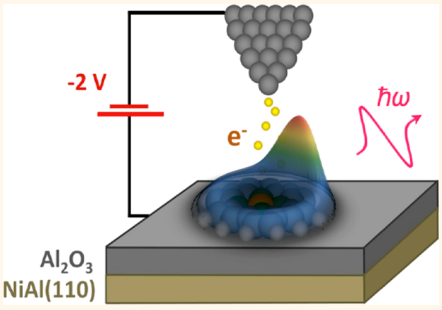

Molecules are quantum matter for which structure is defined by a full specification of quantum numbers for the correlated electron and nuclear motion. Similarly, chemical reactions are transformations of eigenstates of the reactant into those of the reaction products, through multiple pathways that are subject to dynamical constraints.[1,2] The ability of chemists and physicists to interact with atoms, molecules, and solids at the quantum level; on the spatial scales of atoms and chemical bonds; and on temporal scales of electron and nuclear motion has gained increasing sophistication through development of precise photon and electron probes. Yet, even though photon probes have sufficient time resolution to interrogate the electron motion and the sensitivity to monitor the interaction of a single molecule with its environment,[3] in the chemically relevant visible and ultraviolet (UV) range, the wavelength of light is too large to image the structure of single molecules directly. By contrast, electron probes have exquisite spatial resolution, which has enabled imaging of single atoms and atomic lattice contrast on surfaces and in solids, yet traditional electron probes lack the temporal resolution to resolve the nuclear motion. Realizing the limitations and complementary nature of the electron and nuclear probes, a growing trend in chemistry and physics is to marry photon and electron probes by taking advantage of their individual strengths with the ultimate goal of resolving the chemical processes of single molecules or unit cells of solids on the fundamental temporal and spatial scales of electron and nuclear motion. Although impressive advances have been made, the "holy grail" of the universal "chemiscope" remains the subject of intense research based on competing approaches. The article by Lee *et al.* in this issue of *ACS Nano* makes substantial progress toward this goal through submolecular resolution spatial and spectral mapping of electroluminescence from within a single Zn-etioporphyrin radical anion molecule.[4] Inversion of the data using the phase information imprinted by quantum interference between electron scattering channels yields simultaneous sub-Ångstrom spatial and femtosecond temporal resolution of single-molecule reduction–oxidation dynamics. The article by Lee *et al.* is one of a series of publications from the NSF Center for Chemistry at the Space-Time Limit (CaSTL), dedicated to developing and enabling science to interrogate molecular matter with the joint space-time resolution of fundamental relevance to chemistry.

* Address correspondence to petek@pitt.edu.

Published online
10.1021/nn4064538

The "holy grail" of the universal "chemiscope" remains the subject of intense research based on competing approaches.

The unremitting progress toward single-molecule space-time dynamics can be traced to advances in experimental tools for probing the electronic and molecular structure. Herzberg and Porter launched the effort more than 50 years ago by developing flash generation and time-domain probing of transient photochemical products by absorption spectroscopy.[5] Similarly, Müller first imaged single atoms using field ion microscopy.[6] The demonstration of the laser by Maiman[7] and its applications to molecular spectroscopy by Hansch, Schawlow,[8] and others dramatically increased the resolution and sensitivity of molecular probes through the development of spectroscopic methods such as laser-induced fluorescence[9,10] and nonlinear resonant multiphoton ionization.[11] The application of supersonic molecular beam techniques enabled preparation of molecules in well-defined velocity and quantum state distributions and, consequently, the studies of their quantum state-specific unimolecular[2,12] and bimolecular dynamics.[13] Equally important have been the developments in theory, which enabled interpretation of frequency domain spectroscopic data in terms of the implicit time-domain electron and nuclear dynamics.[14,15]

With the development of femtosecond lasers,[16] probing of ensembles of molecules undergoing unimolecular reactions on the time scale of chemical bond evolution along the reaction coordinate, from photoexcited reactant into the product fragments, opened the field of femtochemistry.[17] Similar temporal resolution of the coherent atomic motion in the condensed phase was achieved by applying an abrupt force with an ultrafast laser pulse to launch the coherent phonon oscillations, which could be detected through the Raman tensor as the modulation of the dielectric function of the sample.[18,19] For example, in case of the Si(001) surface, the monitoring of the coherent phonon frequency as a function of delay time reports on the interaction of the lattice with the nonequilibrium photoinduced electron–hole plasma (Figure 1).[19] With the development of attosecond spectroscopy, it is now even possible to time-resolve electron motion in atoms, molecules, and solids on the time scale of the Bohr orbit[20,21] and to couple intense electromagnetic fields with electrons, thereby generating coherent X-ray light.[22] Nevertheless, the wavelength of light in the chemically most relevant IR–UV range fundamentally limits the application of optical methods for microscopy at the atomic scale.

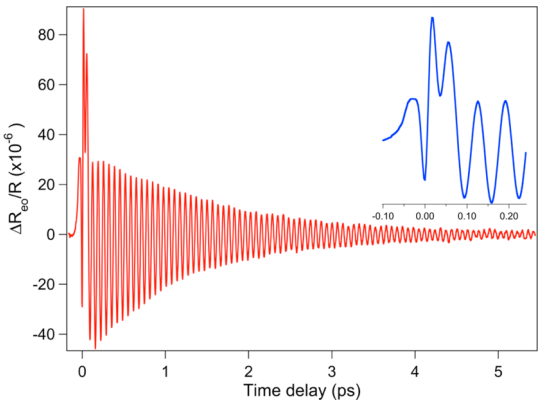

Figure 1. Transient reflectivity from Si measured with <10 fs, 400 nm pump–probe pulses showing modulation due to the electron–hole pair generation near zero delay, and periodic coherent phonon oscillations have an average period of 62 fs, which evolves on the picosecond time scale due to the interaction of the lattice with the photogenerated electron–hole plasma. The inset shows the time-domain Fano interference between the impulsive electronic and oscillatory lattice responses. Reproduced with permission from ref 19. Copyright 2003 Nature Publishing Group.

Electron probes of the structure of matter have achieved equally impressive progress. The de Broglie hypothesis of the dual particle/wave nature of matter was confirmed by diffraction of electrons from crystalline samples,[23] inaugurating powerful methods for structural analysis with atomic-scale resolution. Electron diffraction remains a ubiquitous analytical method for determining atomic-scale structure of surfaces and nanomaterials.[24] Real-space imaging of materials with superior resolution to optical microscopy was developed with the invention of transmission electron microscopy (TEM) by Ruska.[25] Although electrons with <keV energies can probe with sub-Ångstrom resolution, aberration in electron optics required energies in the 100 keV to MeV range for TEM imaging of crystal lattice fringes.[26] The development of optics for correction of the chromatic and spherical aberration triggered a renaissance in TEM methods,[27] enabling imaging of single atoms with element specificity within complex materials and their interfaces, when combined with secondary analytical techniques.[28–30] For example, Figure 2 shows an atomically resolved detail of GaP lattice grown epitaxially on the Si(001) substrate.[31] The growth of polar semiconductor on the neutral substrate leads to the formation of antiphase domains observed in Figure 2 as reversal in the direction of GaP dipoles and formation of a domain boundary.

Another chapter in atom-resolved microscopy was launched through the development of scanning

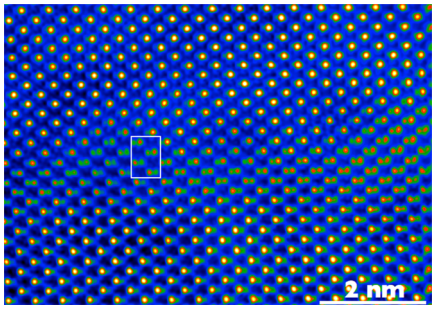

Figure 2. Atomically resolved scanning transmission electron micrograph of a GaP film grown epitaxially on Si(001) substrate (not shown). The GaP dipoles are imaged as asymmetric dumbbells with Ga having the bright contrast. The growth of the polar GaP lattice on neutral Si leads to the formation of antiphase domains with the GaP dipoles pointing in opposite directions on the top and bottom parts of the image. The phase shift in the dipole direction, indicated by the white box and the green contrast in the center of the image, results from the atomically sharp domain boundary. Reproduced with permission from ref 31. Copyright 2013 American Institute of Physics.

tunneling microscopy (STM) by Binnig and Rohrer.[32] Starting with imaging crystalline surfaces, STM rapidly evolved into imaging of single adsorbates;[33] their vibrational spectroscopy by inelastic electron tunneling;[34] the initiation and control of unimolecular, bimolecular, and chain reactions[35−38] and atomic switching.[39] With clever design, it is now possible to switch conductance of single molecules among multiple states by deterministically activating internal vibrations with inelastic electron tunneling.[40] Coupling light into and out of STM tunneling junctions was identified as a potentially powerful method for imaging and probing of single-molecule dynamics[41,42] but until now has met limited success. Atomic force microscopy (AFM) has achieved similarly acute resolution as STM, but by being able to feel forces, it can distinguish the elemental properties of atoms as well as the nature of their chemical bonds.[43,44] Structural probes such as TEM, STM, AFM, and related techniques in their conventional implementations have achieved unsurpassed spatial resolution but lack the temporal resolution for investigating structural dynamics on the fundamental time scales of nuclear motion.

Considering the merits and drawbacks of either photon or electron probes individually, the potential benefits of coupling them to probe ultrafast structure of matter have been appreciated among several communities of chemists and physicists. For example, the femtosecond laser pump−probe delay-time-dependent photoelectron energy and momentum distributions from gas- and liquid-phase molecules obtained in multiphoton photoemission processes provide information about the symmetry and dynamics of electron orbitals as molecules undergo chemical transformations.[45] Similarly, ultrafast multiphoton photoemission spectroscopy has been used to great advantage to study bulk and surface phenomena such as electron dynamics in metals,[46,47] quantum coherence in photon absorption[48] and electron propagation,[49,50] spin polarization,[51] as well as femtochemistry induced by photoinduced charge transfer.[50,52,53] The pump−probe delay dependence of photoemission spectra has enabled, for example, studies of surface femtochemistry of frustrated desorption, electron solvation, and proton-coupled electron transfer.[54−56]

In addition to spectroscopy, ultrafast photoemission techniques are well-suited for microscopy. Here, electron optics image the spatial distribution of photoelectrons emitted from a nanostructured surface in response to an optical pump−probe sequence. By imaging electrons, spatial resolution far below the optical diffraction limit (<10 nm) can be achieved.[57] Time-resolved photoemission electron microscopy has been used to image the excitation, propagation, dephasing, *etc.* of localized and propagating surface plasmons on the femtosecond time scale, as shown in Figure 3.[58−61] Using interferometric techniques, that is, equal-pulse excitation with suboptical cycle (attosecond time scale) delay scanning, one can record movies of the interference patterns between the excitation pulse and the induced plasmon wave packet, which spatially and temporally modulate the two-photon photoemission signal, such as shown for a plasmon interferometer in Figure 3,[58,59] as well as perform coherent control of the plasmon spatiotemporal distributions in nanostructured metallic samples on the nanometer and femtosecond scales.[61,62]

Considering the merits and drawbacks of either photon or electron probes individually, the potential benefits of coupling them to probe ultrafast structure of matter have been appreciated among several communities of chemists and physicists.

Several other embodiments of ultrafast microscopy combine pulsed laser excitation with pulsed electron probing of a solid-state sample.[63−65] The electron pulse is generated by laser-induced photoemission from a photocathode using a portion of the sample excitation pulse, thereby achieving femtosecond time-scale correlation

between the excitation and probing in the sample.[66] These techniques primarily target changes in the atomic structure of the sample in response to the pump pulse through either reciprocal-space electron diffraction[67,68] or real-space electron transmission,[69] but the variety of possible implementations is rapidly increasing. The diffraction techniques, in particular, are exquisitely sensitive to structural changes in response to the optical excitation of the electronic system. For example, crystalline solid–liquid phase transitions have been investigated with subpicosecond resolution for several metals.[64,68] In more complex materials with strong correlation between electrons, phonons, and spins, it is possible to perturb the electronic system to drive electronic phase transitions. For example Figure 4 shows the changes in ultrafast diffraction patterns upon intense femtosecond laser excitation of 1T-TaS_2, which reflect the correlated electron–phonon dynamics in this charge density wave material.[70] In their most established form, the electron probe methods are incorporated into conventional TEM, where laser access to both the photocathode and the sample delivers the ultrafast timing, and the full arsenal of TEM analytical techniques for elemental analysis can be employed. Conventional TEM is not ideally suited for time-resolved measurements, and therefore, such experiments are also starting to be done by building TEM columns from scratch in order to optimize the combined capability for atomically resolved ultrafast measurements.

The major issue for laser pump–electron probe methods, which is a topic of intense research, is the generation and propagation of electron pulses from a photocathode source to the sample with the optimum coherence and pulse duration in order to enable femtosecond time-scale measurements with subatomic resolution. Because electrons are Fermions that interact through Coulomb interactions, this requires either single electron sources or acceleration to relativistic energies, where space-charge effects are ameliorated. The fundamental limitation of photon-pump electron-probe methods, however, is the lack of coherence between the excitation and probing, which

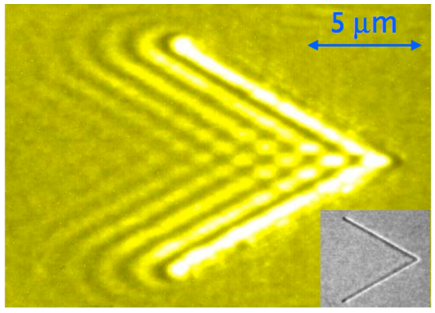

Figure 3. Frame from an attosecond movie showing surface plasmon polariton propagation, interference, and diffraction created by the "V" shaped lithographically formed coupling structure in a silver film. The image shows two-photon photoemission intensity imaged by a photoemission electron microscope upon excitation with identical phase-correlated pump and probe pulses set to a delay of 22.7 fs or 17 optical cycles of the 400 nm light. The inset shows the scanning electron micrograph of the coupling structure, which couples the plasmon into the silver film to create the plasmon interference image.

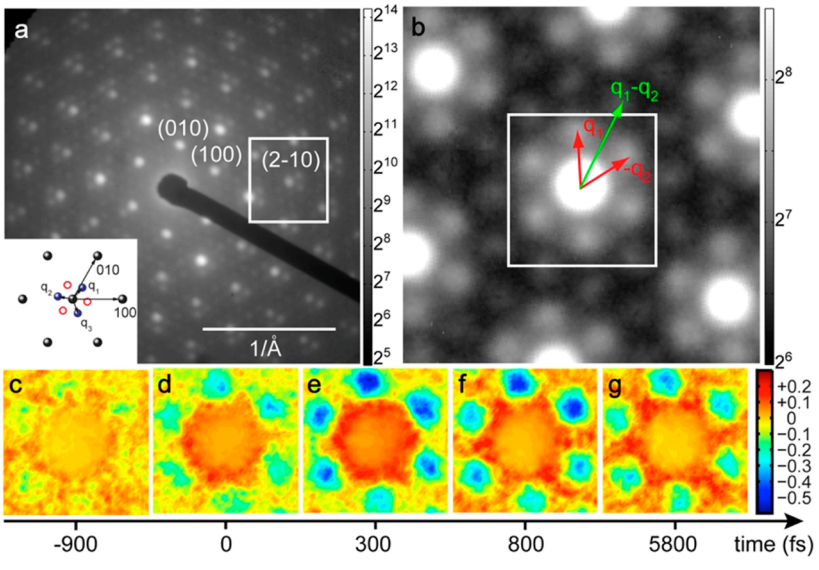

Figure 4. (a) Stationary diffraction pattern of TaS_2 showing the main Bragg peaks of the lattice surrounded by the hexagonal first-order charge density wave (CDW) superstructure (logarithmic intensity scale). (b) Magnified and symmetrized detail of the $(2\bar{1}0)$ Bragg peak. (c–g) Attenuation of the CDW superstructure and intensification of the Bragg peak and their recovery with the delay time are observed upon excitation with intense 3.2 eV, 140 fs laser pulses due to electronically driven atomic motion. Reproduced with permission from ref 70. Copyright 2010 Nature Publishing Group.

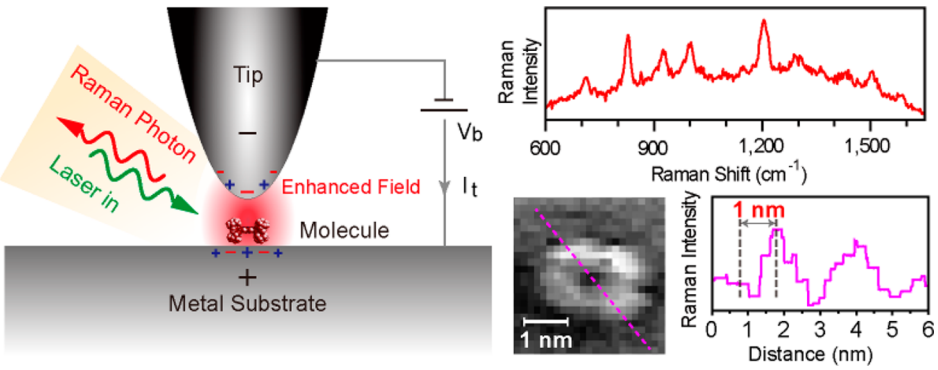

Figure 5. Schematic of the experiment for submolecular resolution Raman imaging, the representative Raman spectrum, and Raman scattering image of a single H_2TBPP molecule with <1 nm resolution. Reproduced with permission from ref 78. Copyright 2013 Nature Publishing Group.

obviates the application of these techniques to coherent quantum phenomena on the nanometer and femtosecond scales.

The most recent trend in ultrafast microscopy, which leads us back to the results of Lee *et al.*,[4] involves coupling scanning probes such as STM, atomic force microscopy (AFM), or near-field microscopy with optical probes.[71] These methods rely on sample structure-dependent interactions with light that are transduced by near-field coupling with a nanometer-scale probe tip.[72] Scanning probe techniques typically employ serial data acquisition for the spatial and temporal coordinates. Therefore, recording three-dimensional (*x*,*y*,*t*) information is time-consuming. Moreover, progress in STM-based approaches has been hampered by laser-pulse-induced heating and consequent thermal expansion of the probe tip,[73] which is often a larger perturbation on the tunneling junction than the laser-field-induced tunneling current. To minimize such limitations, several groups have taken the approach of coupling the light pulse into the shank of the scanning probe and delivering the pulse to the tip as a coherent surface plasmon field with <10 fs duration.[74] Although several experiments have demonstrated high temporal resolution under tunneling conditions,[75−77] none have yet achieved the "holy grail" of resolving single-molecule dynamics.

Two recent experiments that combine light and electron interactions within a STM tip/single-molecule−substrate junction stand out in their promise for achieving the ultimate goal. Recently, Dong and co-workers reported single-molecule Raman scattering with resolution below 1 nm on single *meso*-tetrakis-(3,5-di-*tert*-butylphenyl)porphyrin (H_2TBPP) molecules supported on the Ag(111) surface, as described in Figure 5.[78] The Raman images exhibited resolution on submolecular scales with comparable detail as the simultaneously recorded STM image. Although single-molecule Raman scattering has been demonstrated previously with <10 nm resolution,[79] this is the first achievement of submolecular resolution. Dong and co-workers attribute the resolution to the nonlinear mixing of the broad-band cavity plasmon, which creates a double resonance condition and hence provides the necessary signal enhancement and confines the field to the subnanometer scale to enable submolecular imaging. Moreover, the nonlinear interaction mediated by the cavity plasmon is intrinsically an ultrafast process. The ability to interact with single molecules through the Raman tensor holds promise for ultrafast excitation to create and probe coherent terahertz polarization associated with vibrational modes that are displaced by photo-induced charge transfer within such tip-molecule-surface junctions,[80] in a similar manner as has been possible with solids (Figure 1).[19]

In the report by Lee *et al.*, a further step is taken by extracting time-domain information from electroluminescence that is excited within single Zn-etioporphyrin (ZnEtio) radical anion molecules, which is sandwiched between a STM tip and a thin Al_2O_3 layer formed by oxidizing an NiAl(110) surface.[4] The electroluminescence (EL) spectra recorded by electron tunneling into specific molecular orbitals consist of sharp vibrational features superimposed on a broad continuous background that varies when the tip is tunneling into the orthogonal lobes of the porphyrin molecule. The EL spectra thus reveal submolecular contrast, which Lee *et al.* interpreted in terms of time-dependent electron scattering through different molecular-orbital-specific scattering pathways. Their work gives a rigorous analysis of the combined action of electrons, photons, and plasmons interrogating the coherent inner workings of a single molecule.

In an earlier CaSTL publication, Ho and co-workers demonstrated that EL spectra induced by inelastic scattering of tunneling electrons show vibronic structures that vary with the position of the STM tip above different parts of a single molecule.[81] They used ZnEtio to demonstrate submolecular spatial resolution, and they recognized that the radiative scattering of

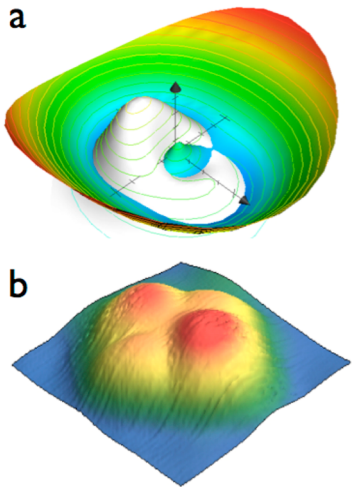

Figure 6. Imaging of correlated electron−nuclear motion of single ZnEtio$^-$ anion through STM-induced electroluminescence. (a) Adiabatic vibronic density (white) at the conical intersection of the Jahn−Teller potential (color map) obtained by direct transformation of the topographic image (b) of the unpaired electron on ZnEtio$^-$. The entanglement between electron and vibrational deformation through the Jahn−Teller Hamiltonian allows the transformation and visualization of the vibrational density, which avoids the singularity of the cone (the cone near the origin of the coordinate system that can be seen to poke through the vibrational density). (a) Reproduced from ref 4. Copyright 2013 American Chemical Society. (b) Reproduced from ref 82. Copyright 2013 American Chemical Society.

tunneling electrons couples to the far-field radiation through the junction plasmon. The information contained within the spectra, however, was unknown and is now elaborated by Lee *et al.* based on their prior analysis of the Jahn−Teller (JT) coupling in the same molecule.[82] In the leading paper, they showed that electron tunneling occurs into the ZnEtio$^-$ negative radical ion, which is stabilized at 5 K on the semi-insulting Al_2O_3 films. Moreover, they showed that the STM topographic images of the anion can be understood as the density of the JT active electron, which can be thought of as an "orbiting orbital" through its coupling to zero-point skeletal deformations of the molecule (Figure 6). Because the electron and pseudorotation of the molecular deformation are entangled through the JT Hamiltonian, the topographic images could be used to image the adiabatic vibrational density of the porphyrin frame. The analysis of the vibrational density showed the avoided singularity of the conical intersection. Their novel interpretation attributes the topographic STM images to portend time-integrated vibronic motion.

Building on this analysis, Lee *et al.* recognize that EL is excited upon injecting a second electron into the molecule, to form the ZnEtio^{2-} dianion. Based on the molecular electronic structure elicited from the scanning tunneling spectra (STS: d*I*/d*V vs V* spectra), the spatial maps of EL, and the spatially resolved EL spectra, they unambiguously assign EL to radiative ionization of the dianion resonance: ZnEtio^{2-} → ZnEtio$^-$ + $h\nu$ + e^-. Because the radiation involves a large dipole in the direction normal to the surface and molecular plane, it is intimately coupled to the radiative modes of the junction plasmon, which greatly enhances the EL yield. Thus, the set of CaSTL papers[4,81,82] illustrates and generalizes principles of submolecular spectroscopy, with spatial resolution that is several orders of magnitude beyond the optical diffraction limit. As in the case of the submolecular resolution Raman imaging,[78] space-frequency domain imaging relies on tunneling into a molecular resonance and plasmon outcoupling. Lee *et al.* take one step further by performing additional space-time analysis through yet another important generalization.

Vibronic resonances, whether in scanning tunneling spectra or in radiative ionization, invariably involve discrete resonances imbedded in a scattering continua. To the extent that the scattering electron can be distinguished as weakly interacting [ZnEtio$^-$ + e^-], the photon emission may be considered to terminate on a shape resonance. In this context, it is possible to contrast the initial radiative dianion state, ZnEtio^{2-}, as a Feschbach resonance, which is longer lived and therefore scattering into this resonance excites the internal vibronic motion. Both resonances are directly observed as sharp STS features with the separation corresponding to the EL photon energy. Quite generally, the quantum interference between continuum and discrete scattering channels leads to dispersive spectral line profiles, commonly known as Fano line shapes.[83] In fact, there is an uncanny similarity between the radiative ionization of ZnEtio^{2-} to similar processes in the decay of the $2p^2$ state of He, which led Majorana to formulate how quantum interferences can appear in atomic spectra[84] and, later, Fano independently to derive his well-known line shape theory.[83]

While it is well-understood that Fano lines contain phase information, this is usually embodied in the coupling strength between the transient state and the continuum. In the case of a Fano progression over a single continuum, Lee *et al.* show that the relative phase can be retrieved. Given relative phases, a vibronic progression completely describes the motion of its generating wave packet. This is illustrated by reconstructing the wave packet motion of the orbiting electron in the shape resonance (Figure 6). As a significant toolset in interpreting Fano line shapes, they give a general procedure for the frequency-time transformation of dispersive interference spectra, and furthermore, they extend the original Fano

formula beyond its original idealization, which assumes that the continuum has a white spectrum. The analysis is insightful, and the extension is widely useful for extracting dynamical information by fitting dispersive spectra. Thus, by expressing the Fano spectrum in terms of a complex line amplitude, $I(\omega) = \mathscr{L}(\omega)\mathscr{L}^*(\omega)$, the amplitude may be transformed to the time domain:

$$\mathscr{L}(t) = (q - i)e^{-\left(i\omega - \frac{\gamma}{2}\right)t} + i\delta(t) \quad (1)$$

where q is the Fano coupling parameter and γ is the lifetime of the transient state. The generating function of the continuum is expressed in eq 1 as a delta function in time, corresponding to an instantaneous scattering process, but Lee *et al.* replace it with a more realistic time correlation function $\delta(t) = (c(t))^{1/2}$ for bound-to-free transitions, given in frequency domain through the reflection approximation:[85]

$$c(\omega) = \int e^{i\omega t}c(t)\mathrm{d}t \sim |V(r(\omega))|^{-1}\varphi^2(r(\omega)) \quad (2)$$

Here, $\phi^2(r)$ is the density of the bound initial state of the electron, and $V(r)$ is the unbound final state potential—a repulsive Coulomb potential screened by the local dielectric, $V(r) = e^2/\varepsilon(r - r_0)$. Lee *et al.* obtain nearly perfect fits of the spectra with the extracted dielectric constant $\varepsilon = 8.5$, in excellent agreement with that of Al_2O_3. The treatment is quite general and should be broadly useful in the analysis of Fano spectra, which arise in diverse settings. Moreover, it emphasizes the physical interpretation of Fano interference in the time domain, which can be seen as the fast modulation near zero delay in the transient reflectivity of Si in the coherent phonon measurement of Figure 1. Such fast transients in the time domain are as common as in the dispersive line shapes in the frequency domain, but the delta function in time, which typically represents the force exerted on the sample by an ultrafast pulse, is often dismissed as a coherent artifact. Thus, as demonstrated by Lee *et al.*, the time- and frequency-domain interpretations of quantum interference are intimately connected, and its analysis either in the frequency or time domain can provide deep insights into quantum mechanical coupling among multiple degrees of freedom in response to electronic excitation.

Beyond the detailed analysis of the elements required for spectroscopy with submolecular spatiotemporal resolution and illustration of the novel information content of such measurements, the paper by Lee *et al.* addresses the inelastic electron scattering resonances observable in the STM junction. Autoionization is pervasive in physics, and dispersive line shapes are ubiquitous. The extension of Lee *et al.* provides both practical tools for analysis and valuable insight in the interpretation of such spectra in time and frequency domain. Furthermore, it highlights the fact that further progress in simultaneous spatial and temporal resolution of single-molecule dynamics requires strong coupling of the electron and photon probes within submolecular volumes. In the case of the work of Lee *et al.*, this coupling is intrinsic to the observed dynamics, and therefore, the observed EL spectra communicate intimate details on the internal processes of the molecular response.

OUTLOOK

To make further progress toward the "holy grail", it is clear that the excitation laser must strongly couple specifically to the molecular electronic and nuclear excitations in order to create response signals in the form of coherently scattered photons or electrons that carry the information on the internal nanometer- and femtosecond-scale dynamics in competition with competing extraneous processes that accompany strong optical fields. Our increased intellectual and experimental ability to interact with single molecules on the fundamental temporal and spatial scales of the electron, nuclear, and other degrees of freedom will enable applications ranging from quantum computing to single-molecule-based electronics.

Conflict of Interest: The authors declare no competing financial interest.

Acknowledgment. The author gratefully acknowledges the financial support for his research on ultrafast microscopy and spectroscopy from the W.M. Keck Foundation and DOE-BES Division of Chemical Sciences, Geosciences, and Biosciences through Grant No. DE-FG02-09ER16056.

REFERENCES AND NOTES

1. Lawrance, W. D.; Moore, C. B.; Petek, H. Understanding Molecular Dynamics Quantum-State by Quantum-State. *Science* **1985**, *227*, 895–901.
2. Moore, C. B. A Spectroscopist's View of Energy States, Energy Transfers, and Chemical Reactions. *Annu. Rev. Phys. Chem.* **2007**, *58*, 1–33.
3. Moerner, W. E. High-Resolution Optical Spectroscopy of Single Molecules in Solids. *Acc. Chem. Res.* **1996**, *29*, 563–571.
4. Lee, J.; Perdue, S. M.; Rodriguez Perez, A.; Apkarian, V. A. Vibronic Motion with Joint Angstrom–Femtosecond Resolution Observed through Fano Progressions Recorded within One Molecule. *ACS Nano* **2013**, 10.1021/nn405335h.
5. Herzberg, G.; Johns, J. W. C. The Spectrum and Structure of Singlet CH_2. *Proc. R. Soc. A* **1966**, *295*, 107–128.
6. Müller, E. W. Resolution of the Atomic Structure of a Metal Surface by the Field Ion Microscope. *J. Appl. Phys.* **1956**, *27*, 474–476.
7. Maiman, T. H. Stimulated Optical Radiation in Ruby. *Nature* **1960**, *187*, 493–494.
8. Schawlow, A. L. Spectroscopy in a New Light. *Rev. Mod. Phys.* **1982**, *54*, 697–707.
9. Zare, R. N.; Dagdigian, P. J. Tunable Laser Fluorescence Method for Product State Analysis. *Science* **1974**, *185*, 739–747.
10. Kinsey, J. L. Laser-Induced Fluorescence. *Annu. Rev. Phys. Chem.* **1977**, *28*, 349–372.
11. Johnson, P. M. Moleculear Multiphoton Ionization Spectroscopy. *Acc. Chem. Res.* **1980**, *13*, 20–26.
12. Nesbitt, D. J.; Field, R. W. Vibrational Energy Flow in Highly Excited Molecules: Role of Intramolecular Vibrational Redistribution. *J. Phys. Chem.* **1996**, *100*, 12735–12756.

13. Neumark, D. M.; Wodtke, A. M.; Robinson, G. N.; Hayden, C. C.; Lee, Y. T. Molecular Beam Studies of the $F+H_2$ Reaction. *J. Chem. Phys.* **1985**, *82*, 3045–3066.
14. Heller, E. J. Time-Dependent Approach to Semiclassical Dynamics. *J. Chem. Phys.* **1975**, *62*, 1544–1555.
15. Frederick, J. H.; Heller, E. J.; Ozment, J. L.; Pratt, D. W. Ring Torsional Dynamics and Spectroscopy of Benzophenone: A New Twist. *J. Chem. Phys.* **1988**, *88*, 2169–2184.
16. Shank, C. V.; Ippen, E. P. Subpicosecond Kilowatt Pulses from a Mode-Locked CW Dye Laser. *Appl. Phys. Lett.* **1974**, *24*, 373–375.
17. Zewail, A. H. Femtochemistry: Atomic-Scale Dynamics of the Chemical Bond. *J. Phys. Chem. A* **2000**, *104*, 5660–5694.
18. Dhar, L.; Rogers, J. A.; Nelson, K. A. Time-Resolved Vibrational Spectroscopy in the Impulsive Limit. *Chem. Rev.* **1994**, *94*, 157–193.
19. Hase, M.; Kitajima, M.; Constantinescu, A. M.; Petek, H. The Birth of a Quasiparticle in Si Observed in Time-Frequency Space. *Nature* **2003**, *426*, 51.
20. Corkum, P. B.; Krausz, F. Attosecond Science. *Nat. Phys.* **2007**, *3*, 381–387.
21. Cavalieri, A. L.; Muller, N.; Uphues, T.; Yakovlev, V. S.; Baltuska, A.; Horvath, B.; Schmidt, B.; Blumel, L.; Holzwarth, R.; Hendel, S.; *et al.* Attosecond Spectroscopy in Condensed Matter. *Nature* **2007**, *449*, 1029–1032.
22. Popmintchev, T.; Chen, M.-C.; Popmintchev, D.; Arpin, P.; Brown, S.; Ališauskas, S.; Andriukaitis, G.; Balčiunas, T.; Mücke, O. D.; Pugzlys, A.; *et al.* Bright Coherent Ultrahigh Harmonics in the keV X-ray Regime from Mid-infrared Femtosecond Lasers. *Science* **2012**, *336*, 1287–1291.
23. Davisson, C.; Germer, L. H. Diffraction of Electrons by a Crystal of Nickel. *Phys. Rev.* **1927**, *30*, 705–740.
24. Van Hove, M. A. Atomic-Scale Structure: From Surfaces to Nanomaterials. *Surf. Sci.* **2009**, *603*, 1301–1305.
25. Knoll, M.; Ruska, E. Das Elektronenmikroskop. *Z. Phys.* **1932**, *78*, 318–339.
26. Kawasaki, T.; Yoshida, T.; Matsuda, T.; Osakabe, N.; Tonomura, A.; Matsui, I.; Kitazawa, K. Fine Crystal Lattice Fringes Observed Using a Transmission Electron Microscope with 1 MeV Coherent Electron Waves. *Appl. Phys. Lett.* **2000**, *76*, 1342–1344.
27. Haider, M.; Uhlemann, S.; Schwan, E.; Rose, H.; Kabius, B.; Urban, K. Electron Microscopy Image Enhanced. *Nature* **1998**, *392*, 768–769.
28. Chu, M.-W.; Chen, C. H. Chemical Mapping and Quantification at the Atomic Scale by Scanning Transmission Electron Microscopy. *ACS Nano* **2013**, *7*, 4700–4707.
29. Boyes, E. D.; Ward, M. R.; Lari, L.; Gai, P. L. ESTEM Imaging of Single Atoms under Controlled Temperature and Gas Environment Conditions in Catalyst Reaction Studies. *Ann. Phys.* **2013**, *525*, 423–429.
30. Zhou, W.; Oxley, M. P.; Lupini, A. R.; Krivanek, O. L.; Pennycook, S. J.; Idrobo, J.-C. Single Atom Microscopy. *Microsc. Microanal.* **2012**, *18*, 1342–1354.
31. Beyer, A.; Haas, B.; Gries, K. I.; Werner, K.; Luysberg, M.; Stolz, W.; Volz, K. Atomic Structure of (110) Antiphase Boundaries in GaP on Si(001). *Appl. Phys. Lett.* **2013**, *103*, 032107.
32. Binning, G.; Rohrer, H.; Gerber, C.; Weibel, E. Surface Studies by Scanning Tunneling Microscopy. *Phys. Rev. Lett.* **1982**, *49*, 57–61.
33. Baró, A. M.; Binnig, G.; Rohrer, H.; Gerber, C.; Stoll, E.; Baratoff, A.; Salvan, F. Real-Space Observation of the 2×1 Structure of Chemisorbed Oxygen on Ni(110) by Scanning Tunneling Microscopy. *Phys. Rev. Lett.* **1984**, *52*, 1304–1307.
34. Lauhon, L. J.; Ho, W. Single-Molecule Vibrational Spectroscopy and Microscopy: CO on Cu(001) and Cu-(110). *Phys. Rev. B* **1999**, *60*, R8525.
35. Hla, S.-W.; Meyer, G.; Rieder, K.-H. Inducing Single-Molecule Chemical Reactions with a UHV-STM: A New Dimension for Nano-Science and Technology. *ChemPhysChem* **2001**, *2*, 361–366.
36. Ho, W. Single-Molecule Chemistry. *J. Chem. Phys.* **2002**, *117*, 11033–11061.
37. Kim, Y.; Komeda, T.; Kawai, M. Single-Molecule Reaction and Characterization by Vibrational Excitation. *Phys. Rev. Lett.* **2002**, *89*, 126104.
38. Maksymovych, P.; Sorescu, D. C.; Jordan, K. D.; Yates, J. T., Jr. Collective Reactivity of Molecular Chains Self-Assembled on a Surface. *Science* **2008**, *322*, 1664–1667.
39. Eigler, D. M.; Lutz, C. P.; Rudge, W. E. An Atomic Switch Realized with the Scanning Tunneling Microscope. *Nature* **1991**, *352*, 600–603.
40. Huang, T.; Zhao, J.; Feng, M.; Popov, A. A.; Yang, S.; Dunsch, L.; Petek, H. A Multi-state Single-Molecule Switch Actuated by Rotation of an Encapsulated Cluster within a Fullerene Cage. *Chem. Phys. Lett.* **2012**, *552*, 1–12.
41. Berndt, R.; Gaisch, R.; Schneider, W. D.; Gimzewski, J. K.; Reihl, B.; Schlittler, R. R.; Tschudy, M. Atomic Resolution in Photon Emission Induced by a Scanning Tunneling Microscope. *Phys. Rev. Lett.* **1995**, *74*, 102.
42. Wu, S. W.; Ogawa, N.; Ho, W. Atomic-Scale Coupling of Photons to Single-Molecule Junctions. *Science* **2006**, *312*, 1362–1365.
43. Sugimoto, Y.; Pou, P.; Abe, M.; Jelinek, P.; Perez, R.; Morita, S.; Custance, O. Chemical Identification of Individual Surface Atoms by Atomic Force Microscopy. *Nature* **2007**, *446*, 64–67.
44. Gross, L.; Mohn, F.; Moll, N.; Schuler, B.; Criado, A.; Guitián, E.; Peña, D.; Gourdon, A.; Meyer, G. Bond-Order Discrimination by Atomic Force Microscopy. *Science* **2012**, *337*, 1326–1329.
45. Suzuki, T. Time-Resolved Photoelectron Spectroscopy of Non-adiabatic Electronic Dynamics in Gas and Liquid Phases. *Int. Rev. Phys. Chem.* **2012**, *31*, 265–318.
46. Bokor, J. Ultrafast Dynamics at Semiconductor and Metal Surfaces. *Science* **1989**, *246*, 1130–1134.
47. Petek, H.; Ogawa, S. Femtosecond Time-Resolved Two-Photon Photoemission Studies of Electron Dynamics in Metals. *Prog. Surf. Sci.* **1997**, *56*, 239–310.
48. Petek, H.; Heberle, A. P.; Nessler, W.; Nagano, H.; Kubota, S.; Matsunami, S.; Moriya, N.; Ogawa, S. Optical Phase Control of Coherent Electron Dynamics in Metals. *Phys. Rev. Lett.* **1997**, *79*, 4649–4652.
49. Höfer, U.; Shumay, I. L.; Reuss, C.; Thomann, U.; Wallauer, W.; Fauster, T. Time-Resolved Coherent Photoelectron Spectroscopy of Quantized Electronic States on Metal Surfaces. *Science* **1997**, *277*, 1480.
50. Ge, N.-H.; Wong, C. M.; Lingle, R. L.; McNeill, J. D.; Gaffney, K. J.; Harris, C. B. Femtosecond Dynamics of Electron Localization at Interfaces. *Science* **1998**, *279*, 202–205.
51. Winkelmann, A.; Lin, W.-C.; Bisio, F.; Petek, H.; Kirschner, J. Interferometric Control of Spin-Polarized Electron Populations at a Metal Surface Observed by Multiphoton Photoemission. *Phys. Rev. Lett.* **2008**, *100*, 206601.
52. Ogawa, S.; Nagano, H.; Petek, H. Phase and Energy Relaxation in an Anti-bonding Surface State: Cs/Cu-(111). *Phys. Rev. Lett.* **1999**, *82*, 1931–1934.
53. Güdde, J.; Berthold, W.; Höfer, U. Dynamics of Electronic Transfer Processes at Metal/Insulator Interfaces. *Chem. Rev.* **2006**, *106*, 4261–4280.
54. Petek, H.; Weida, M. J.; Nagano, H.; Ogawa, S. Real-Time Observation of Atomic Motion above a Metal Surface. *Science* **2000**, *288*, 1402–1404.
55. Stähler, J.; Bovensiepen, U.; Meyer, M.; Wolf, M. A Surface Science Approach to Ultrafast Electron Transfer and Solvation Dynamics at Interfaces. *Chem. Soc. Rev.* **2008**, *37*, 2180–2190.
56. Li, B.; Zhao, J.; Onda, K.; Jordan, K. D.; Yang, J.; Petek, H. Ultrafast Interfacial Proton-Coupled Electron Transfer. *Science* **2006**, *311*, 1436–1440.
57. Locatelli, A.; Bauer, E. Recent Advances in Chemical and Magnetic Imaging of Surfaces and Interfaces by XPEEM. *J. Phys.: Condens. Matter* **2008**, *20*, 093002.
58. Kubo, A.; Onda, K.; Petek, H.; Sun, Z.; Jung, Y. S.; Kim, H. K. Femtosecond Imaging of Surface Plasmon Dynamics in a Nanostructured Silver Film. *Nano Lett.* **2005**, *5*, 1123–1127.

59. Kubo, A.; Pontius, N.; Petek, H. Femtosecond Microscopy of Surface Plasmon Polariton Wave Packet Evolution at the Silver/Vacuum Interface. *Nano Lett.* **2007**, *7*, 470–475.
60. Aeschlimann, M.; Brixner, T.; Fischer, A.; Kramer, C.; Melchior, P.; Pfeiffer, W.; Schneider, C.; Strüber, C.; Tuchscherer, P.; Voronine, D. V. Coherent Two-Dimensional Nanoscopy. *Science* **2011**, *333*, 1723–1726.
61. Winkelmann, A.; Tusche, C.; Unal, A. A.; Chiang, C.-T.; Kubo, A.; Wang, L.; Petek, H. In *Dynamics of Interfacial Electron and Excitation Transfer in Solar Energy Conversion: Theory and Experiment*; Piotrowiak, P., Ed.; Royal Society of Chemistry: Cambridge, 2013.
62. Kubo, A.; Jung, Y. S.; Kim, H. K.; Petek, H. Femtosecond Microscopy of Localized and Propagating Surface Plasmons in Silver Gratings. *J. Phys. B* **2007**, *40*, S259.
63. Mourou, G.; Williamson, S. Picosecond Electron Diffraction. *Appl. Phys. Lett.* **1982**, *41*, 44–45.
64. Siwick, B. J.; Dwyer, J. R.; Jordan, R. E.; Miller, R. J. D. An Atomic-Level View of Melting Using Femtosecond Electron Diffraction. *Science* **2003**, *302*, 1382–1385.
65. Lobastov, V. A.; Srinivasan, R.; Zewail, A. H. Four-Dimensional Ultrafast Electron Microscopy. *Proc. Natl. Acad. Sci. U.S.A.* **2005**, *102*, 7069–7073.
66. Reed, B. W.; Armstrong, M. R.; Browning, N. D.; Campbell, G. H.; Evans, J. E.; LaGrange, T.; Masiel, D. J. The Evolution of Ultrafast Electron Microscope Instrumentation. *Microsc. Microanal.* **2009**, *15*, 272–281.
67. Ruan, C.-Y.; Murooka, Y.; Raman, R. K.; Murdick, R. A.; Worhatch, R. J.; Pell, A. The Development and Applications of Ultrafast Electron Nanocrystallography. *Microsc. Microanal.* **2009**, *15*, 323–337.
68. Sciaini, G.; Miller, R. J. D. Femtosecond Electron Diffraction: Heralding the Era of Atomically Resolved Dynamics. *Rep. Prog. Phys.* **2011**, *74*, 096101.
69. Zewail, A. H. 4D Ultrafast Electron Diffraction, Crystallography, and Microscopy. *Annu. Rev. Phys. Chem.* **2006**, *57*, 65–103.
70. Eichberger, M.; Schafer, H.; Krumova, M.; Beyer, M.; Demsar, J.; Berger, H.; Moriena, G.; Sciaini, G.; Miller, R. J. D. Snapshots of Cooperative Atomic Motions in the Optical Suppression of Charge Density Waves. *Nature* **2010**, *468*, 799–802.
71. Xu, X. G.; Raschke, M. B. Near-Field Infrared Vibrational Dynamics and Tip-Enhanced Decoherence. *Nano Lett.* **2013**, *13*, 1588–1595.
72. Jones, A. C.; O'Callahan, B. T.; Yang, H. U.; Raschke, M. B. The Thermal Near-Field: Coherence, Spectroscopy, Heat-Transfer, and Optical Forces. *Prog. Surf. Sci.* **2013**, *88*, 349–392.
73. Gerstner, V.; Thon, A.; Pfeiffer, W. Thermal Effects in Pulsed Laser Assisted Scanning Tunneling Microscopy. *J. Appl. Phys.* **2000**, *87*, 2574.
74. Berweger, S.; Atkin, J. M.; Xu, X. G.; Olmon, R. L.; Raschke, M. B. Femtosecond Nanofocusing with Full Optical Waveform Control. *Nano Lett.* **2011**, *11*, 4309–4313.
75. Lee, J.; Perdue, S. M.; Whitmore, D.; Apkarian, V. A. Laser-Induced Scanning Tunneling Microscopy: Linear Excitation of the Junction Plasmon. *J. Chem. Phys.* **2010**, *133*, 104706.
76. Terada, Y.; Yoshida, S.; Takeuchi, O.; Shigekawa, H. Real-Space Imaging of Transient Carrier Dynamics by Nanoscale Pump-Probe Microscopy. *Nat. Photonics* **2010**, *4*, 869–874.
77. Dey, S.; Mirell, D.; Perez, A. R.; Lee, J.; Apkarian, V. A. Nonlinear Femtosecond Laser Induced Scanning Tunneling Microscopy. *J. Chem. Phys.* **2013**, *138*, 154202.
78. Zhang, R.; Zhang, Y.; Dong, Z. C.; Jiang, S.; Zhang, C.; Chen, L. G.; Zhang, L.; Liao, Y.; Aizpurua, J.; Luo, Y.; *et al.* Chemical Mapping of a Single Molecule by Plasmon-Enhanced Raman Scattering. *Nature* **2013**, *498*, 82–86.
79. Pozzi, E. A.; Sonntag, M. D.; Jiang, N.; Klingsporn, J. M.; Hersam, M. C.; Van Duyne, R. P. Tip-Enhanced Raman Imaging: An Emergent Tool for Probing Biology at the Nanoscale. *ACS Nano* **2013**, *7*, 885–888.
80. Jorn, R.; Zhao, J.; Petek, H.; Seideman, T. Current-Driven Dynamics in Molecular Junctions: Endohedral Fullerenes. *ACS Nano* **2011**, *5*, 7858–7865.
81. Chen, C.; Chu, P.; Bobisch, C. A.; Mills, D. L.; Ho, W. Viewing the Interior of a Single Molecule: Vibronically Resolved Photon Imaging at Submolecular Resolution. *Phys. Rev. Lett.* **2010**, *105*, 217402.
82. Lee, J.; Perdue, S. M.; Perez, A. R.; El-Khoury, P. Z.; Honkala, K.; Apkarian, V. A. Orbiting Orbitals: Visualization of Vibronic Motion at a Conical Intersection. *J. Phys. Chem. A* **2013**, *117*, 11655–11664.
83. Fano, U. Effects of Configuration Interaction on Intensities and Phase Shifts. *Phys. Rev.* **1961**, *124*, 1866.
84. Arimondo, E.; Clark, C. W.; Martin, W. C. Colloquium: Ettore Majorana and the Birth of Autoionization. *Rev. Mod. Phys.* **2010**, *82*, 1947–1958.
85. Heller, E. J. Quantum Corrections to Classical Photodissociation Models. *J. Chem. Phys.* **1978**, *68*, 2066–2075.